In-situ Construction of Multi-hierarchical CdS-DETA/$In(OH)_3$/Ag_2S Dual-S-Scheme Heterojunction for Accurate Depolymerizing the β-O-4 Bond in Lignin Compound

Zhi-yu Liang[a], Gui-yang Yan[a], Er-da Zhan[b], Guo-xin Zhuang[c*], Ying Wang[a*], Qiao-ling Mo[d]

[a] Fujian Provincial Key Laboratory of Featured Materials in Biochemical Industry, College of New Energy and Materials, Ningde Normal University, Fujian 352100, China

[b] college of Chemistry, Fuzhou University, 2 Xueyuan Road, University New District, Fuzhou 350108, China.

[c] Scientific Research and Experiment Center, Fujian Police College, No. 59 Shoushan Road, Fuzhou, 350007, Fujian, China

[d] Center of Analysis and Testing, Nanchang University, 999 Xuefu Avenue, Nanchang, Jiangxi Province, 330031, China.

*Corresponding author. E-mail: gx_zhuang@fjpsc.edu.cn

wy891203@163.com

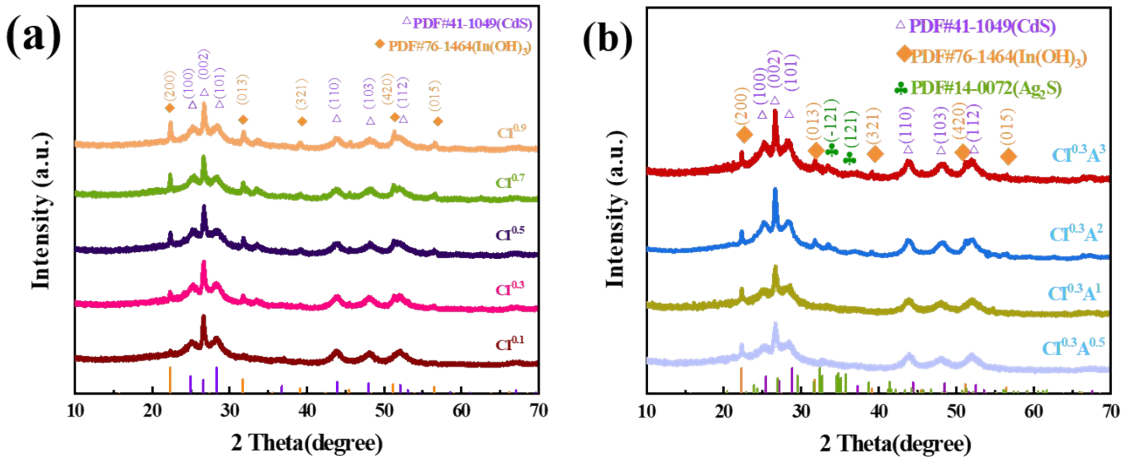

Figure s1. XRD patterns of as-prepared (a) CdS-DETA/$In(OH)_3$ composites, and (b) CdS-DETA/$In(OH)_3$/Ag_2S composites.

Table s1. BET parameters of CdS-DETA, $CI^{0.3}$ and $CI^{0.3}A^2$ heterojunction.

Samples	**BET surface area (m^2/g)**	**Pore volume (cm^2/g)**	**Pore size (nm)**
CdS-DETA	47.02	0.25	13.81
$CI^{0.3}$	77.87	0.39	16.83
$CI^{0.3}A^2$	66.07	0.32	15.30

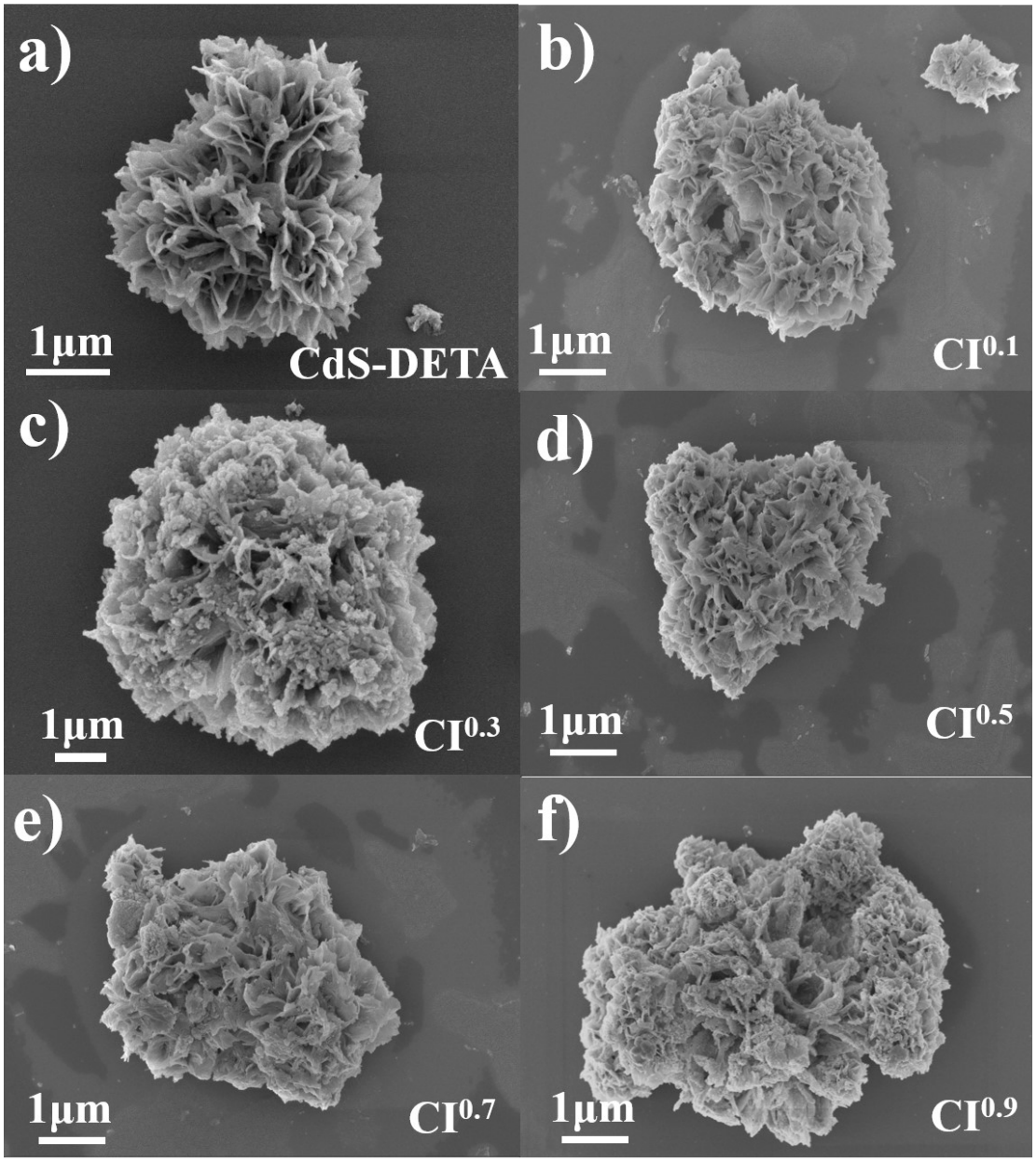

Figure s2. SEM images of as-prepared CdS-DETA/$In(OH)_3$ composites.

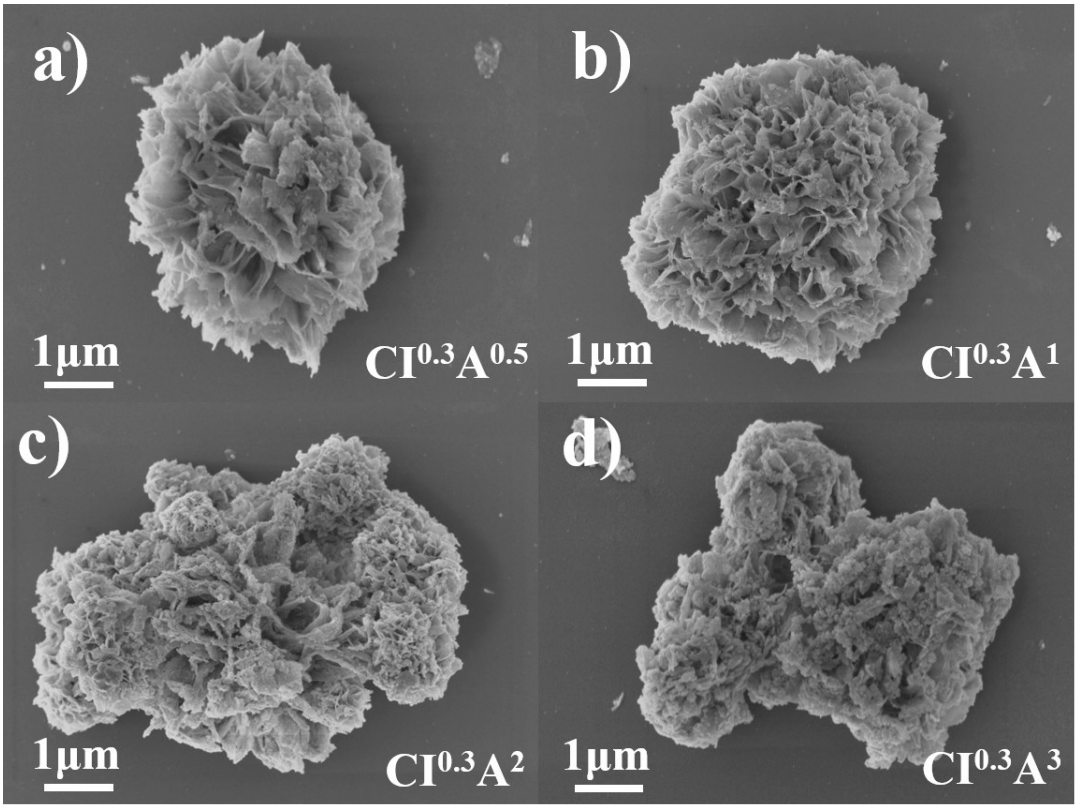

Figure s3. SEM images of as-prepared CdS-DETA/$In(OH)_3$/Ag_2S composites.

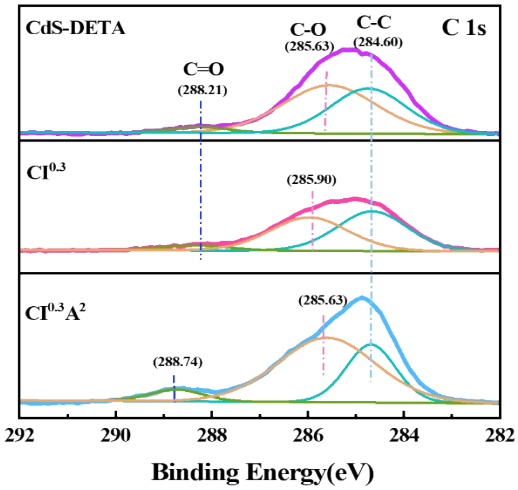

Figure s4. C 1s high-resolution spectra of CdS-DETA, $CI^{0.3}$ and $CI^{0.3}A^{2}$.

Table s2. XPS binding energies of the as-synthesized photocatalysts.

Element	CdS-DETA	$CI^{0.3}$	$CI^{0.3}A$	Chemical bond species
C 1s	284.60	284.60	284.60	C-C
C 1s	285.63	285.90	285.63	C-O
C 1s	288.21	288.21	288.74	C=O
S $2p_{1/2}$	162.50	162.50	163.13	S^{2-}
S $2p_{3/2}$	161.22	161.22	161.73	S^{2-}
Cd $3d_{3/2}$	411.22	411.55	412.06	Cd^{2+}
Cd $3d_{5/2}$	404.48	404.80	405.29	Cd^{2+}
In $3d_{3/2}$	N/A	452.10	452.02	In^{3+}
In $3d_{5/2}$	N/A	444.54	445.07	In^{3+}
Ag $3d_{3/2}$	N/A	N/A	373.97	Ag^{+}
Ag $3d_{5/2}$	N/A	N/A	367.94	Ag^{+}

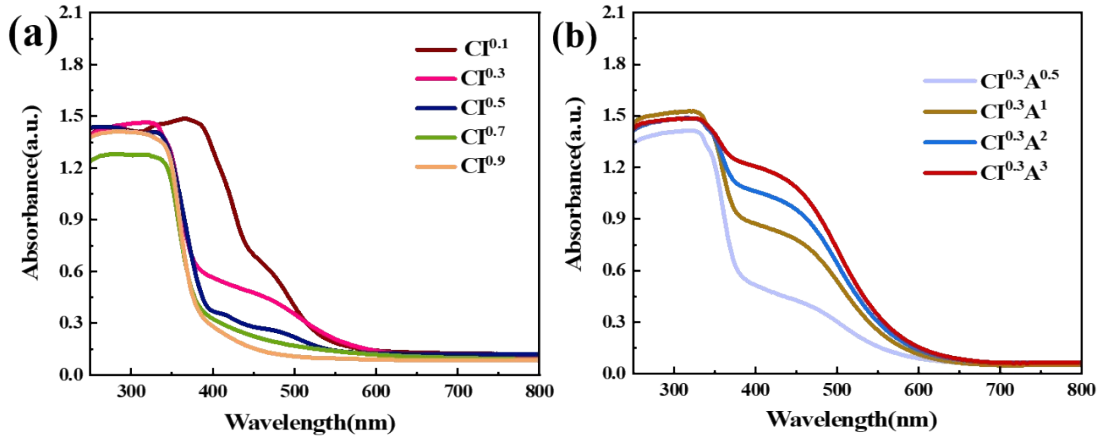

Figure s5. UV-Vis absorption spectra of (a) CdS-DETA/$In(OH)_3$ composites, and (b) CdS-DETA/$In(OH)_3$/Ag_2S composites.

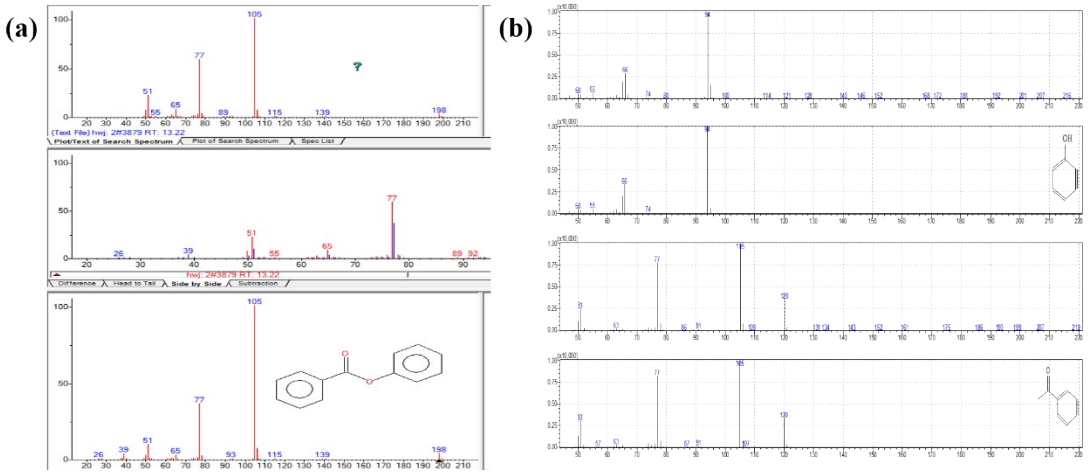

Figure s6. GC-MS spectra for photocatalytic depolymerization of PP-ol conversion over $CI^{0.3}A^{2}$.

Table s3. Comparison of the $CI^{0.3}A^2$ photocatalyst with reported photocatalysts.

Materials	Light source	Solvent	Photocatalytic efficiency (mmol $h^{-1}g^{-1}$)*	Ref.
CdS QDs	300 W Xe lamp	CH_3CN	3.33	*1*
Ni/CdS	Blue LEDs	CH_3CN/0.1 M KOH (v/v = 2/8).	0.8	*2*
ZIS-3	Xe lamp	CH_3CN:H_2O (v/v = 2/3)	3.3	*3*
CdS-C_3N_4	Blue LEDs	CH_3CN/H_2O (v/v = 4/1)	5	*4*
CdS−SH/TiO_2	300 W Xe lamp	CH_3CN	0.5	*5*
30% CN/ZIS	300 W Xe lamp	CH_3CN:H_2O(v/v = 2/3)	2.3	*6*
$ZnIn_2S_4$	9.6 W blue LEDs (455 nm)	CH_3CN	4.5	*7*
Zn_4In_2S	Xe lamp (400-780 nm), 0.6 W/cm^2	CH_3CN/H_2O (v/v=1)	2.05	*8*
$CI^{0.3}A^2$	300 W Xe lamp	CH_3CN:H_2O(v/v = 1/2)	6.67	This work

*Photocatalytic efficiency (mmol·h^{-1}·g^{-1}) = Yield of Products/ (Reaction time×Catalyst amount)

Table s4. Photocatalytic depolymerization efficiency of $CI^{0.3}A^{2}$ towards different β-O-4 model compounds.

Entry	Substrate	Conversion (%)	Yield (%)	
1	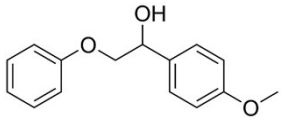	93	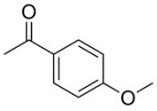 66	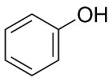 82
2	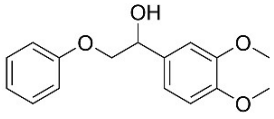	93	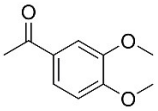 64	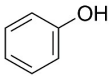 79
3	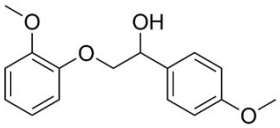	92	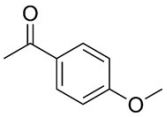 58	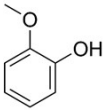 75
4	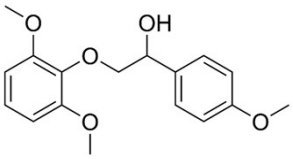	88	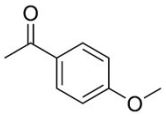 60	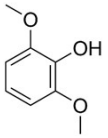 76

*Reaction conditions: lignin model compound (10 mg), catalyst (1 mg), acetonitrile solution ($V_{water}/V_{acetonitrile}$ =1/2, 1.0 ml), N_2 (1 atm), and 300 W xenon lamp.

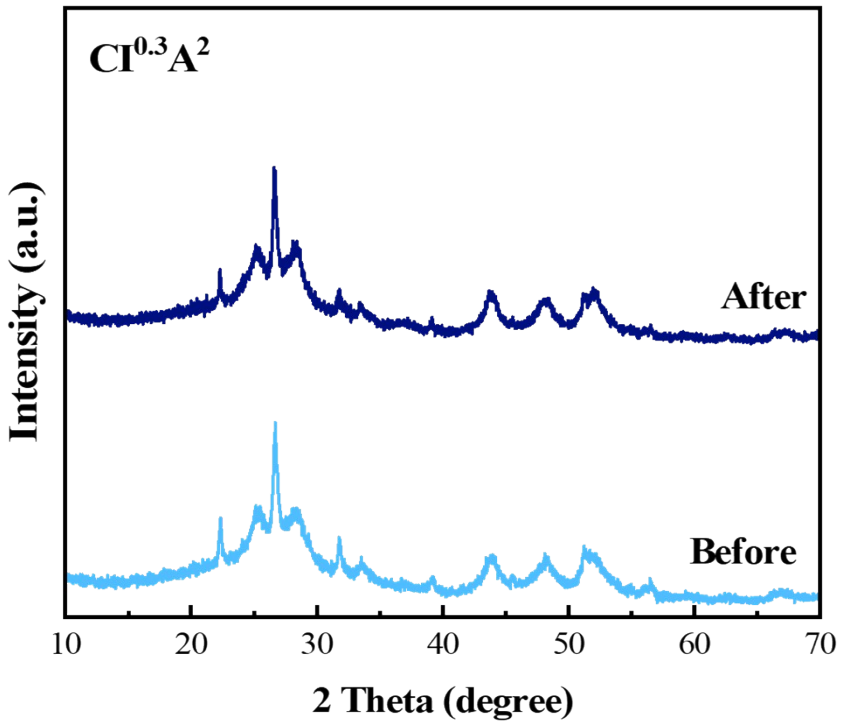

Figure s7. XRD pattern of $CI^{0.3}A^2$ before and after the cycling experiment on the conversion of PP-ol.

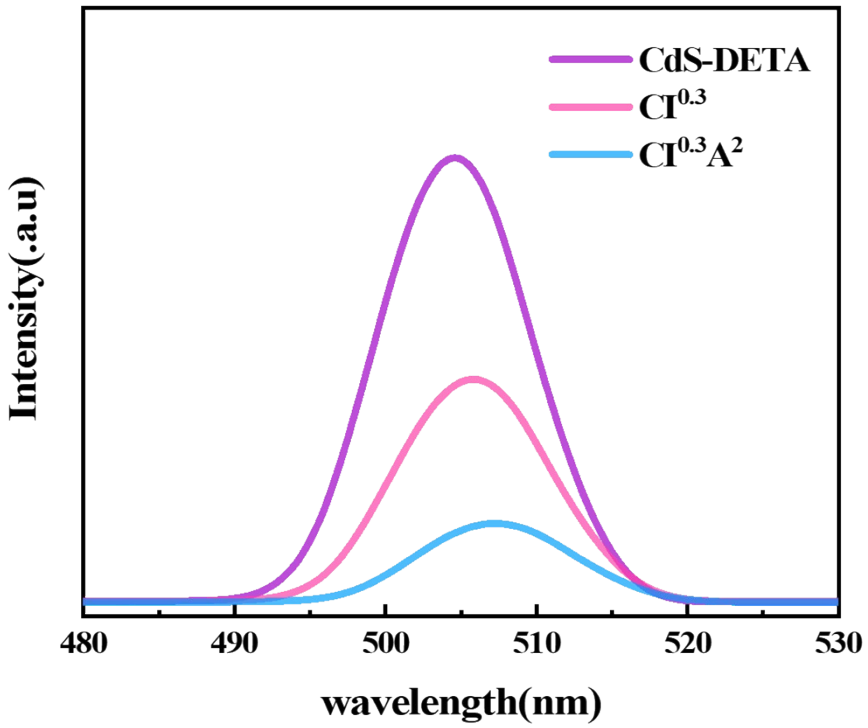

Figure s8. PL spectra of CdS-DETA, $CI^{0.3}$ and $CI^{0.3}A^2$. (λ_{ex}=325 nm)

DFT Methods

The first-principles tool-Vienna Ab initio Simulation Package(VASP) [9, 10] was employed to perform all density functional theory (DFT) calculations within the generalized gradient approximation (GGA) using the Perdew-Burke-Ernzerhof (PBE) [11] formulation. We have chosen the projected augmented wave (PAW) potentials [12, 13] to describe the ionic cores and take valence electrons into account using a plane wave basis set with a kinetic energy cutoff of 450 eV. Partial occupancies of the Kohn-Sham orbitals were allowed using the Gaussian smearing method and a width of 0.05 eV. For the optimization of both geometry and lattice size, the Brillouin zone integration was performed with 0.04 /Å *Γ*-centered *k*-point sampling [14]. The self-consistent calculations applied a convergence energy threshold of 10^{-5} eV. The equilibrium geometries and lattice constants were optimized with maximum stress on each atom within 0.02 eV $Å^{-1}$. The weak interaction was described by DFT+D3 method using empirical correction in Grimme's scheme [14]. Spin polarization method was adopted to describe the magnetic system.

Reference

[1] X. J. Wu, X. T. Fan, S. J. Xie, J. C. Lin, J. Cheng, Q. H. Zhang, L. Y. Chen and Y. Wang, Solar energy-driven lignin-first approach to full utilization of lignocellulosic biomass under mild conditions, ***Nat. Catal.***, 1(10) (2018) 772-780.

[2] G. Han, T. Yan, W. Zhang, Y. C. Zhang, D. Y. Lee, Z. Cao and Y. Sun, Highly selective photocatalytic valorization of lignin model compounds using ultrathin metal/CdS, ***ACS Catal.***, 9(2019) 11341-11349.

[3] S. Shao, K. Wang, J. B. Love, J. Yu, S. Du, Z. Yue and X. Fan, Water promoted photocatalytic C_β-O bonds hydrogenolysis in lignin model compounds and lignin biomass conversion to aromatic monomers, ***Chem. Eng. J.***, 435 (2022) 134980.

[4] J. Y. Wang, Z. Z. Hu, X. T. Sun, Y. Q. Gao, J. L. Wang, J. Xu and G. Jin, Highly dispersed CdS on C_3N_4 for selective cleavage of C_β-O-4 bonds in lignin model compound under blue light, ***Surf. Interfaces***, 36 (2023) 102505.

[5] S. Xu, Q. Gao, Z. Y. Hu, Y. T. Lu, Y. L. Qin and Y. L. Li, CdS-SH/TiO_2 heterojunction photocatalyst significantly improves selectivity for C-O bond breaking in lignin models, ***ACS Catal.***, 13 (2023) 13941-13954.

[6] X. T. Liu, Z. J. Jiang, X. R. Cao, Z. Shen, W. Zhao, F. Wang, M. Y. Cui and C. Liang, Fabrication of s-scheme g-C_3N_4/$Zn_4In_2S_7$ heterojunction photocatalyst for enhancing selective cleavage of β-O-4 bond in lignin model compounds and lignin, ***ACS Sustain. Chem. Eng.***, 11(2023) 14947-14959.

[7] N. Luo, M. Wang, H. Li, J. Zhang, T. Hou, H. Chen, X. Zhang, J. Lu, F. Wang, visible-light-driven self-hydrogen transfer hydrogenolysis of lignin models and extracts into phenolic products, ***ACS Catal.***, 7 (2017) 4571-4580.

[8] J. Lin, X. Wu, S. Xie, L. Chen, Q. Zhang, W. Deng, Y. Wang, visible-light-driven cleavage of C-O linkage for lignin valorization to functionalized aromatics, ***ChemSusChem.***, 12 (2019) 5023-5031.

[9] G. Kresse, J. Furthmüller, Efficiency of Ab-initio total energy calculations for metals and semiconductors using a plane-wave basis set. ***Comput. Mater. Sci.***, 6 (1996) 15-50.

[10] G. Kresse, J. Furthmüller, Efficient iterative schemes for Ab Initio total-energy calculations using a plane-wave basis set. ***Phys. Rev. B***, 54 (1996) 11169-11186.

[11] J. P. Perdew , K. Burke, M. Ernzerhof, Generalized gradient approximation made simple. ***Phys. Rev. Lett.***, 77 (1996) 3865-3868.

[12] G. Kresse, D. Joubert, From ultrasoft pseudopotentials to the projector Augmented-Wave method. ***Phys. Rev. B***, 59 (1999) 1758-1775.

[13] P. E. Blöchl, Projector Augmented-Wave method. ***Phys. Rev. B***, 50 (1994) 17953-17979.

[14] H. J. Monkhorst, J. D. Pack, Special points for Brillouin-zone integrations[J]. ***Phys. Rev. B***, 13(1976): 5188.